

Fatigue life prediction of hoist drum-rail contact pair based on digital twin

Michael A Zhuravkov^{a,c}, Mikhail A Nikolaitchik^{b,c}, Zengcheng Wang^{a,c}, Guangbin Yu^{a,c,*}

^a School of Mechatronics Engineering, Harbin Institute of Technology, Harbin, 150001, China

^b Theoretical and Applied Mechanics Department, Belarusian State University, Minsk 220030, Belarus

^c Heilongjiang Provincial Key Laboratory of Gear Transmission for Sea and Air Equipment, Harbin 150001, China

ARTICLE INFO

Keywords:

Digital twin
Fatigue wear
Mechanical-mathematical model
Monitoring

ABSTRACT

Application of digital twin development technology allows to significantly improve safety and reduce operational costs of complex technical systems. The detailed description of the mine lifting complex elements digital twin development process is presented. In particular the geotechnical system “roller of the lifting vessel - mine conductor” digital twin is considered. The developed digital twin allows to determine the moving lifting vessel on mine conductors contact interaction forces in real time using data from the motion smoothness monitoring system. The obtained forces values allow us to calculate both the current conductors under the influence of the moving lifting vessel stress-strain state and the number of cycles “descent-lift” to conductors fatigue wear. A cycle of experimental studies on contact-mechanical fatigue of the system under consideration was performed. The contact load was increased stepwise according to the proposed loading scheme until significant values of plastic deformation, vibration and noise occurred. Modification of the mechanical-mathematical model of contact wear is performed. The variation of the normal load as a function of the loading cycle is taken into account. The developed mechanical-mathematical model of multi-cycle digital twin wear is verified by the experimental investigations and can be refined with a set of statistics of the considered physical object observations. The digital twin developed makes it possible to provide additional monitoring of the mine shaft steel structures under various operating conditions state, which makes it possible to rely not only on visual monitoring means. The proposed technology of mine shaft DT development allows to rapidly make important technical decisions on controlling the operation of critical elements of the geotechnical system considered (modes of operation, repair and replacement, etc.). This fact not only minimizes costs, but also ensures safe operation of the geotechnical system under consideration. The solutions developed were tested and implemented in the practice of one of the operating mining enterprises and showed their high efficiency.

1. Introduction

A digital twin (DT) of some object can be defined as a digital (virtual, computer) dynamic intellectual model of this object with a large set of input information and data from various sensors, devices and experts. Digital twins also comprise a layer of behavioral insights and visualizations derived from data [1]. Put simply, a digital twin is a “virtual replica” of a physical object, person, or technological or natural process that can be used to simulate its behavior to better understand “how it functions in reality, in real life” [2]. It is assumed, that DT reproduces the form, characteristic features and properties, behavior and state of its physical prototype (object) according to a set of specified parameters, properties, criteria. It is obvious that the greater the number of determining parameters and properties of an object its DT takes into account,

the more adequate and close it is to the original. Thus, the ideology of creating a DT requires the inclusion of information and data from various sensors, instruments, and experts in the virtual model in addition to the original information [3]. According to the main goals and objectives, the DT is required for modeling and computer simulation of the state and behavior of the physical original under various conditions of influence on it. For example, in the automotive industry, DTs are changing how new cars are designed, tested, and built. Automotive manufacturers use DTs to create a virtual representation of a new car model, which allows them to optimize the safety and efficiency of each vehicle without having to invest in multiple costly physical prototypes [4].

Today, a large number of publications are devoted to the solution of mechanics applied problems using digital twin technology. Thus, the

* Corresponding author.

E-mail address: 3482235817@qq.com (G. Yu).

<https://doi.org/10.1016/j.rineng.2025.105271>

Received 1 April 2025; Received in revised form 6 May 2025; Accepted 9 May 2025

Available online 13 May 2025

2590-1230/© 2025 The Authors. Published by Elsevier B.V. This is an open access article under the CC BY license (<http://creativecommons.org/licenses/by/4.0/>).

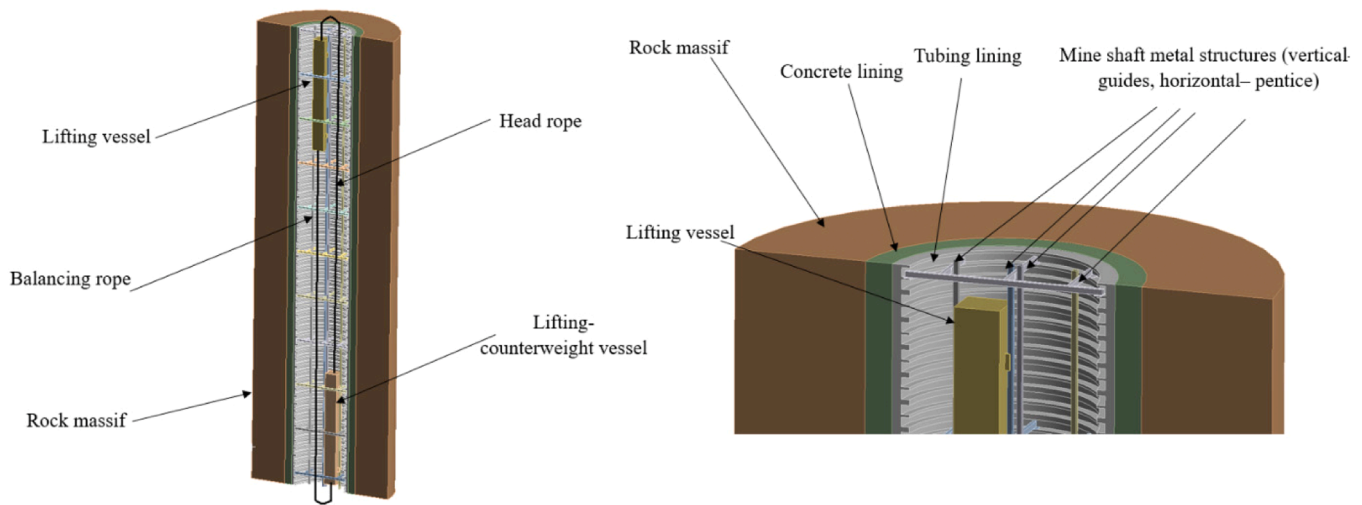


Fig. 1. Scheme of geotechnical system "mine shaft - rock massif".

CFD problem is solved using hybrid twins: digital and virtual twins [5]. In researches by Liu and Gui the DT technology is applied to solve robotics problems [6,7]. DT technologies together with DEM are applied to describe the state of the ball bearing [8]. Also, digital twins are used in the development of power windows design in the study [9]. In addition, the application of DT technology has been widely used in modeling of complex multi-element technical systems [10,11].

The mine shaft belongs to the category of particularly critical geotechnical structures requiring high attention. Ensuring the predictable and accident-free operation of mine shafts is critical not only for the mining company's employees performing "descents and ascents" guaranteed safety, but also for the safe operation of underground structures and ensuring stable economic parameters of the mining enterprise.

In addition, the mine shaft consists of many elements which are concrete lining in contact with the surrounding rock massif; tubing lining; a system of metal structures that provide the motion of lifting vessels along the shaft; the lifting vessel itself with guide rollers and a system of lifting ropes (Fig. 1).

Mine lifting complex represent an important element of mining enterprise with the underground method of mining. Lifting complexes are complex engineering and technical structures, the efficiency and safety of which is generally ensured by the reliable and trouble-free operation of its individual elements, components and systems. One of the most critical systems of the mine lifting complex is the lifting vessel complex with the corresponding additional equipment. Ensuring trouble-free and optimal operation of a lifting vessel is a complex task that requires solving a large set of mechanical problems. The complexity of solving this problem is determined by the fact that the subject of the study is a multi-element system (the lifting vessel itself, guiding conductors, metal structures, mine shaft reinforcement, ropes network and many other element) operating in a multivariate mode. A large number of authors have been researching this issue for a long time [12–15]. An important element of the lifting vessel is the contact group "lifting vessel roller – mine conductors". Most researchers consider this problem from the point of view of only theoretical mechanics or the mechanics of a deformable solid or experimental approaches [16,17].

2. Wear stress analysis of a roller shaft system based on DT

Let's consider the process of "mine shaft lifting vessel roller – mine conductor" system digital twin construction by developing specialized mechanical and mathematical models of considering system behavior as well as "tuning" the DT through experimental studies of tribological pair "roller – shaft" contact interaction and wear.

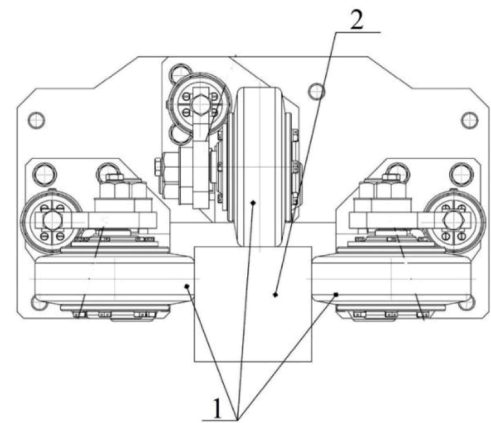


Fig. 2. Rollers and conductors contact node: 1 – lifting vessel rollers; 2 – conductor.

As a basic model we consider a finite element model of rollers with a conductor contact interaction during the motion of a cargo lifting vessel used for lifting rock and bulk cargoes to the earth surface.

An example of the technical system element under study is presented in Fig. 2. A system of three rollers (1) located on different sides of the conductor moves along the conductor. The motion of a lifting vessel in a mine shaft is most often limited by two or less often by four conductors.

The following contact interaction conditions are taken into account during the finite element simulation:

Linear contact which assumes the absence of sliding and separation between contacting bodies surfaces (Bonded type);

Nonlinear contact which assumes the slippage between contacting bodies (sliding conditions), while the friction coefficient is zero and the normal pressure takes on a zero value in case of separation (Frictionless type);

Contact with friction when the tangential stresses arise in the contact area between bodies upon reaching a limiting value the bodies slide relative to each other (Frictional type).

The equations of bilinear isotropic theory of elasticity [18] are accepted as the law of materials behavior. This approach makes it possible to take into account elastoplastic effects. In the bilinear theory the elasticity section is described by Young's modulus and Poisson's ratio. The plasticity section is described by yield stress and the yield surface angle of inclination. The numerical characteristics of the quantities in the contact area of the bodies under consideration are chosen as

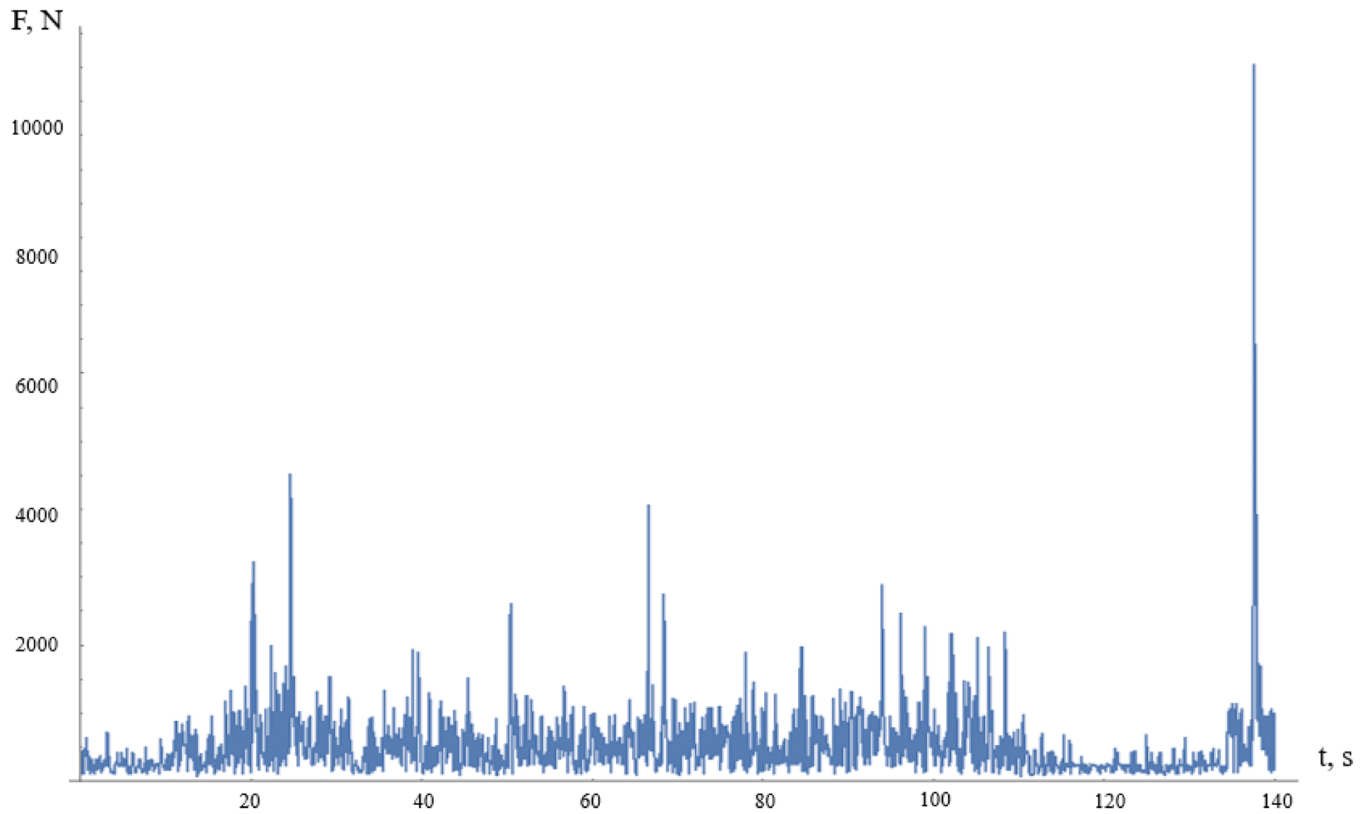


Fig. 3. Graph of the force impact of a lifting vessel on a conductor during one lift.

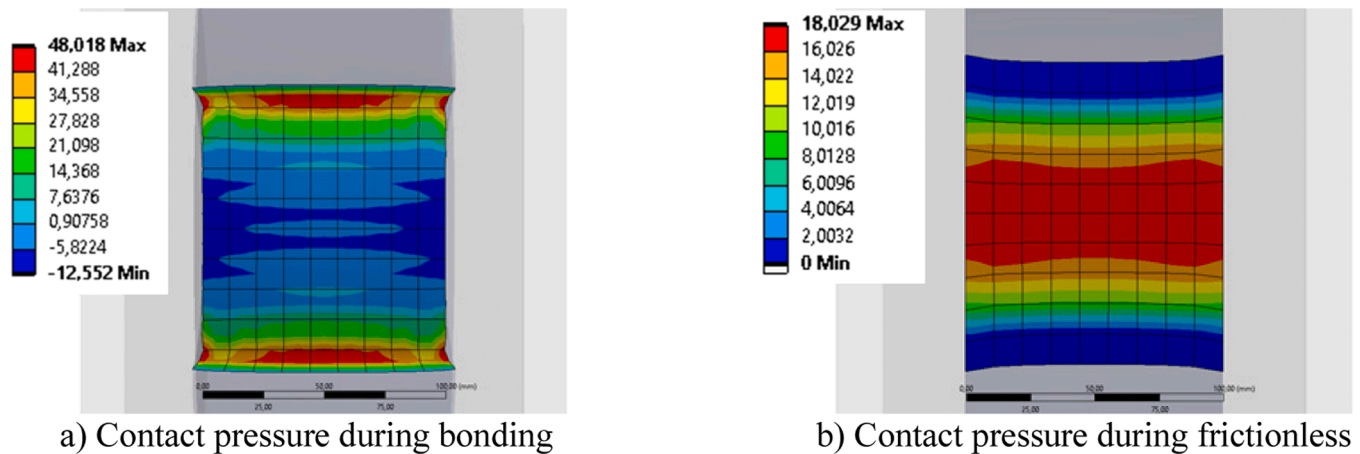


Fig. 4. Contact pressure for different contact types, MPa.

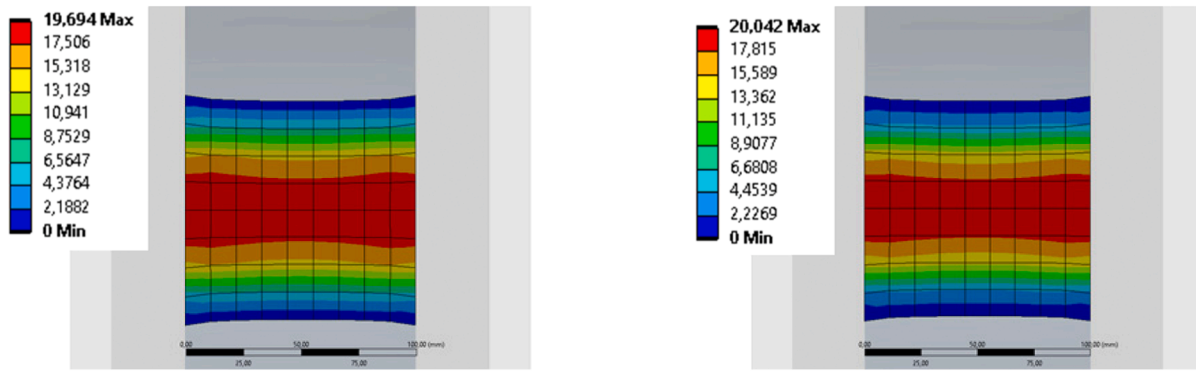
follows: yield strength – 250 MPa, yield surface inclination angle – 0 degrees.

To determine the magnitude of the contact load transmitted through the spring-loaded rollers to the conductors, as well as the position of the rollers in real time, a developed algorithm is used to calculate the magnitude of the lifting vessel on the conductors force impact using a system for monitoring mine lifting vessel motion smoothness [19,20]. Fig. 3 shows a graph of the lifting vessel on the conductor force impact during 1 lift, obtained from accelerometer readings.

The materials of the DT elements is adopted as follows: conductor – steel; the roller is steel rubberized on the outside, so average values of the constants were chosen: $E_1 = 200$ GPa, $E_2 = 180$ MPa are steel and rubber Young's modulus respectively. Poisson's ratio is 0.49 for the rubber and 0.3 for the steel.

The following characteristic geometric parameters of bodies are used when constructing a finite element model. Roller outer diameter is 320 mm, inner diameter is 200 mm, roller width is 100 mm. The conductor has box-shaped cross-section. 200 mm and 164 mm are the outer square and inner square lengths of the conductor respectively. The length of the conductor is 6000 mm. The analytical solution used to verify the numerical solutions obtained on the basis of the DT finite element model is constructed on the basis of the classical Hertz solution [21,22].

Figs. 4, 5 show the pressure distribution in the contact area. In the case of bodies complete contact stress concentration zones are located along the edges of the contact surface. The maximum contact pressure is observed in the center of the contact area and its value increases with increasing friction coefficient between the interacting bodies in the case of incomplete contact. This fact corresponds to real contact interaction.



a) Contact pressure with a friction coefficient of 0.1 b) Contact pressure with a friction coefficient of 0.3

Fig. 5. Contact pressure for different friction coefficient, MPa.

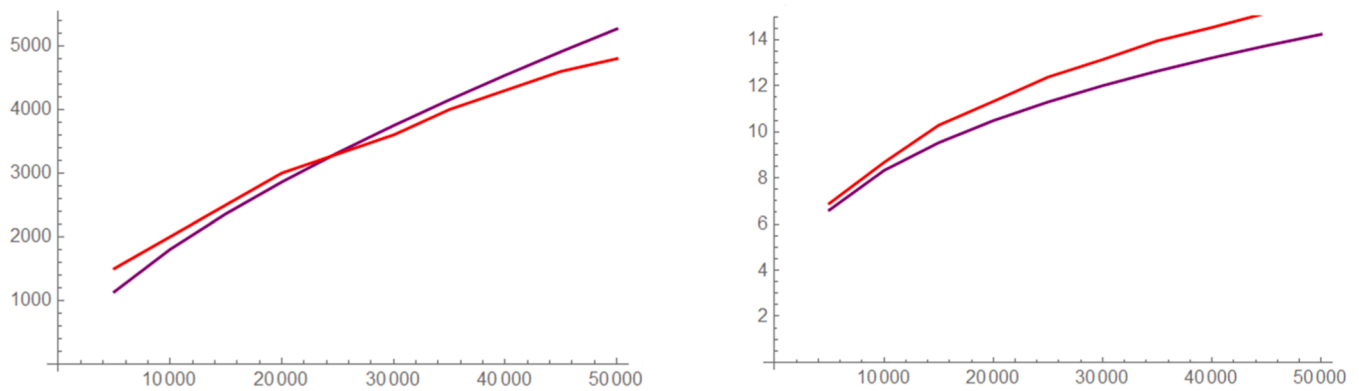


Fig. 6. Comparison of the contact patch area as well as the maximum contact pressure depending on the applied load obtained by computer modeling (red) and using analytical solution (purple).

Fig. 6 shows the contact patch area and maximum contact pressure calculated using the analytical solution and the results of computer modelling. The discrepancies in the results of calculating the contact patch area and the maximum contact pressure according to the analytical solution and the results of numerical modeling do not exceed 10 % as follows from the Fig. 6.

The finite element model of contact interaction presented as part of the development of “lifting vessel roller – mine conductor” system DT can be used further to assess the durability of mine conductors. Durability here refers to the fatigue failure of conductors under the influence of repeatedly variable (cyclic) loads that arise during the lifting vessel motion. Both the interaction of an individual roller with a conductor and a system of two rollers are considered when carrying out fatigue analysis. The problem of studying the contact conditions influence on the number of cycles until fatigue failure of the structure is solved during numerical modelling of the DT fatigue wear. The possibility of roller and conductor interaction both in one plane (contact of one roller with the conductor) and in two planes (contact of two rollers with the conductor) is taken into account.

The choice of the from zero loading cycle is caused by the fact that such a loading cycle allows to avoid negative values of loads (case of the conductor force impact on the rollers), the occurrence of which is impossible during the operation of the considered geotechnical system. During the rollers of the lifting vessel force action on the conductors the magnitude of the interaction forces varies from zero to the maximum loading value determined by the results of the monitoring system data processing [19,20].

The material fatigue properties are usually determined by the tests

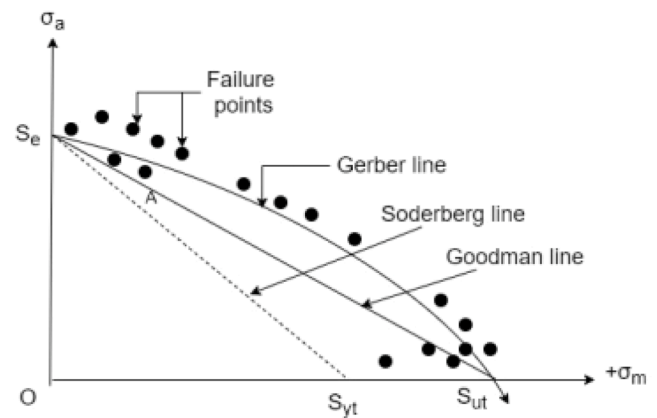


Fig. 7. Graphs of mean stress correction methods equations.

using a symmetrical stress cycle with constant amplitude. In-service components are rarely subjected to this type of load in practice. On the other hand conducting tests for different mean stresses or stress ratios can be inefficient and very expensive. There are empirical methods for the mean stress correction in such a case. The following methods were considered and analyzed during the research [23]:

- Goodman method $S_{ca} = \frac{S_a}{1 - (S_{mean}/S_{ut})}$;
- Gerber method $S_{ca} = \frac{S_a}{1 - (S_{mean}/S_{ut})^2}$;

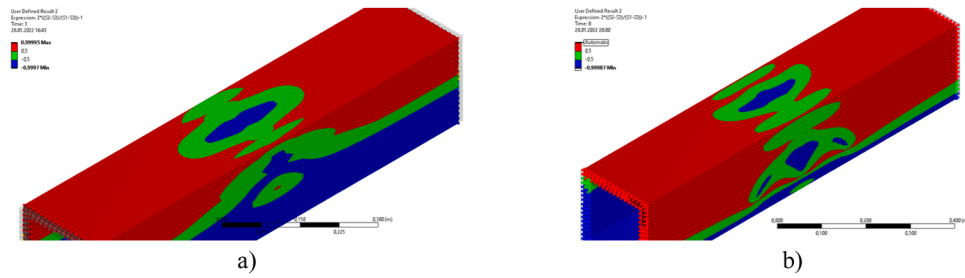


Fig. 8. Distribution of the Nadai-Lode coefficient in the contact zone for the frictional type of contact interaction with the friction coefficient of 0.3: a) – for one roller; b) – for two rollers.

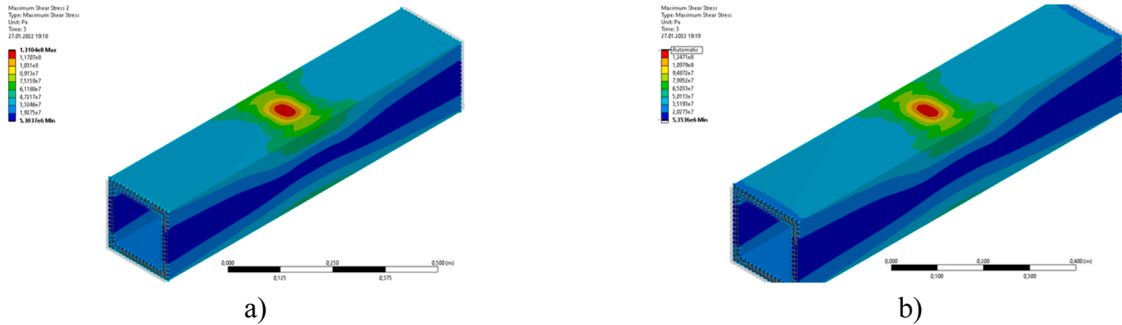


Fig. 9. Maximum shear stresses when one roller acts on a conductor: a) – frictionless contact type; b) – frictional contact type with the friction coefficient of 0.3.

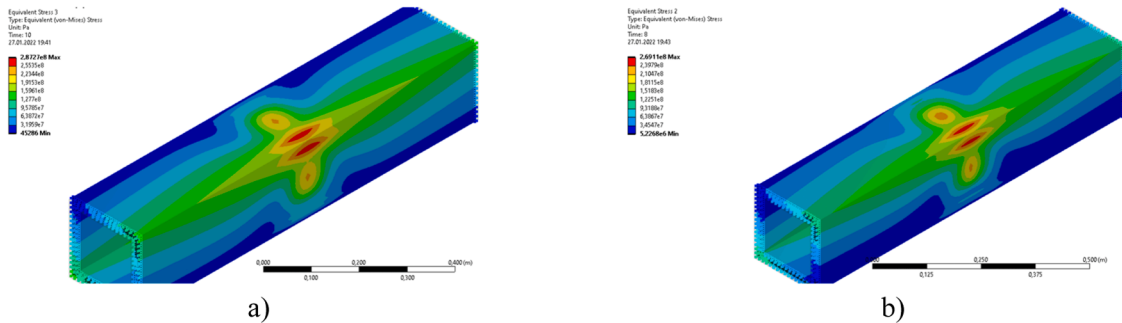


Fig. 10. Equivalent stresses when two rollers act on the conductor: a) – frictionless contact type; b) – frictional contact type with the friction coefficient of 0.3.

(c). Soderberg method $S_{ca} = \frac{S_a}{1 - (S_{mean}/S_y)}$,

where S_y is the yield strength; S_{ca} is the corrected variable stress; S_{mean} is the mean stress; S_u is the tensile strength.

Fig. 7 shows a graphical interpretation of the mean stress correction methods shown above.

In Fig. 7 are used next symbol: σ_a is alternating stress (stress amplitude), σ_m is mean stress, S_{yt} is yield strength, S_{ut} is ultimate strength, S_e is stress amplitude after mean stress correction. The dotted line indicates the beginning of the plasticity zone. The Goodman, Soderberg and Gerber lines limit the values of the graph below with fatigue failure does not occur. Failure points lying outside the Goodman, Soderberg and Gerber lines indicate that fatigue failure will occur at such values according to the selected mean stress correction criterion. These methods

are used for stress levels correction, allowing the stress cycles to be compared with the standard S-N curve obtained for a symmetric stress cycle.

We use the Nadai-Lode coefficient in order to select the type of stresses by which the fatigue of the structure was assessed [24]:

$$\mu = 2 \frac{(\sigma_2 - \sigma_3)}{(\sigma_1 - \sigma_3)} - 1 \quad (1)$$

Nadai-Lode parameter varies in the interval from “-1” to “1” and characterizes the type of volumetric stress state:

$\mu_\sigma \in [-1; -0,5]$ corresponds to the state of generalised tension;

$\mu_\sigma \in [-0,5; 0,5]$ corresponds to the state of generalized shear;

$\mu_\sigma \in [0,5; 1]$ corresponds to the state of generalised compression.

The modelling results show that tensile and shear stresses prevail in the stress concentration region for both types of contact interaction

Table 1

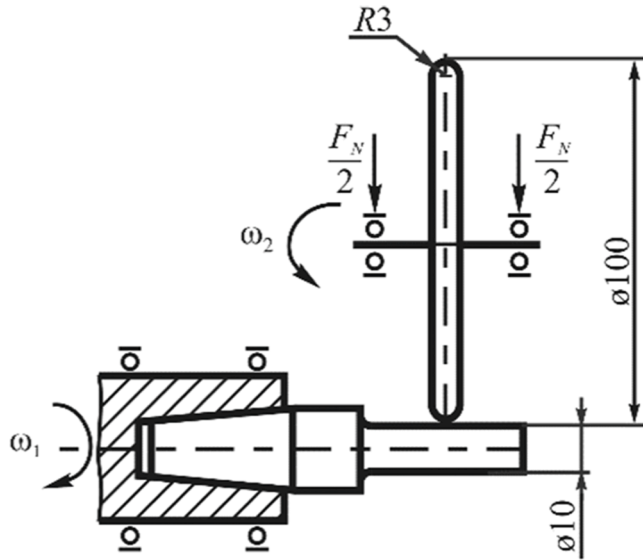
Comparison of the cycles number to fatigue failure of a conductor in interaction with one roller.

Contact type	Frictionless	Frictionless	Frictional	Frictional
Stress component	Equivalent stress	Maximum shear stress	Equivalent stress	Maximum shear stress
Number of cycles	53480	35335	41495	25406

Table 2

Comparison of the cycles number to fatigue failure of a conductor in interaction with two rollers.

Contact type	Frictionless	Frictionless	Frictional	Frictional
Stress component	Equivalent stress	Maximum shear stress	Equivalent stress	Maximum shear stress
Number of cycles	59176	40631	13736	94902

**Fig. 11.** Test scheme.

considered (Fig. 8). Therefore, we also choose tangential in addition to equivalent stresses as stresses for the conductor fatigue assessment. Figs. 9, 10 show some results of a numerical experiments performed.

As an example, Tables 1 and 2 show the number of cycles to fatigue failure of a conductor when it interacts with one and two rollers using the Goodman mean stress correction method respectively.

The results of system under consideration DT wear numerical simulations allowed us to draw conclusions of applied importance for the assessment of conductor condition during the mine lifting vessel motion. Specifically:

- (1) When a single roller interacts with the conductor, the following relationship is observed. When friction is taken into account, the number of cycles to fatigue failure of the conductor decreases significantly for any combination of mean stress and stress component correction methods;
- (2) When two rollers interact with the conductor, the number of cycles to fatigue failure decreases comparing to the number of cycles values when the conductor interacts with a single roller;
- (3) The number of cycles before fatigue cracks occur in the conductor for the case of contact with friction is greater than for contact without friction when two rollers impact the conductor. This is caused by the fact that the zone of stress concentration and, as a consequence, the area of fatigue crack initiation is the contact zone of the roller with the conductor in the case of interaction with a single roller. Therefore, the stress concentration in the contact zone increases as the friction coefficient increases. At the same time, the fatigue wear initiation region is outside the contact zone in the case of impact from two rollers. Thus, when the friction coefficient increases the values of deformations and, as a consequence, stresses in the zone of their maximum concentration decrease in the case of contact of a conductor with two rollers.

3. Analysis of the actual state of the roller shaft system

The system “roller – shaft” was chosen as the basic physical object describing the considered interaction due to the complexity of the lifting vessel rollers with mine conductors interaction continuous monitoring, as well as the duration of the contact wear process.

Contact-mechanical fatigue tests were carried out for the “roller-shaft” system, made of steel 25CrMnTi (roller) and steel C45 (shaft) respectively. The properties of 25CrMnTi steel were selected as follows: endurance limit $\sigma_{-1} = 570\text{MPa}$, contact fatigue limit $p_f = 3100\text{MPa}$. Properties of steel C45 were selected as follows: $\sigma_{-1} = 260\text{MPa}$, $p_f = 1760\text{MPa}$.

A characteristic feature of this force system is that the strength of the shaft metal is substantially less than the roller, so that the tests only reveal residual deformation and damage in the vicinity of the raceway on the shaft, while the dimensions of the roller remain virtually undistorted.

The test scheme as well as the test protocol of the investigated system are shown in Figs. 11 and 12.

The bending force in the experiments $Q = 225\text{N} = \text{const}$ corresponds to a stress amplitude of $\sigma_a(225\text{MPa}) < \sigma_{-1}(260\text{MPa})$. The contact load is varied stepwise according to the loading program shown in Fig. 12. The contact endurance limit $p_f = 1760\text{MPa}$ was exceeded at the III stage of loading.

During the tests, the roller motion on the shaft entered a non-stationary regime when it moved from stage VII to stage VIII of contact loading, i.e. after 700 000 test cycles (see arrow 1 in Fig. 12). The residual radial deformations of the shaft in the unsteady zone are shown in Fig. 12 by the light dots (750 154 loading cycles, i.e., in the middle of stage VIII). At stage IX there was a loss of motion stability (see arrow 2 in Fig. 12). The residual radial deformation of the shaft at loss of motion stability is shown in Fig. 13 by crosses (851 688 loading cycles, i.e. in the middle of stage IX). Test discontinued at X stage at = 976 100 load cycles due to unacceptable vibrations and noise $N_{\Sigma} = 976\,100$ load cycles due to unacceptable vibrations and noise. The residual shaft deformations as a number of cycles function are shown in Fig. 13.

The main features of shaft damage observed by the results of experimental studies are as follows. Several specific frozen waves of surface plastic deformations were formed on the contact surface. They are a set of irregular, semi-barrel-shaped wells. None of the holes are repeated and each of them has its own different dimensions in all three directions (radial, axial, circumferential) that differ from the others. The value of relative plastic deformation (under the conditions of this experiment) reaches 10 % in radial and 30 % in axial directions.

4. Analysis of wear strain values in roller-shaft systems based on digital twin

As a part of a physical object with a digital twin interaction the problem of a conductor under the influence of a constant normal load multi-cycle contact wear was solved. The effect of partial fretting on the bodies contact interaction was taken into account [27]. The initial and final configurations of the roller and conductor contact area in the considered model problem are shown in Fig. 14.

In the Fig. 14 a_0 is half-width of the entire initial contact zone, c_* is half-width of the stick zone, a_{∞} is the limit half-width of the contact zone, P is the normal load, Q_* is the tangential load.

The analytical solution of the formulated modelling problem was based on the approach proposed by Argatov [27].

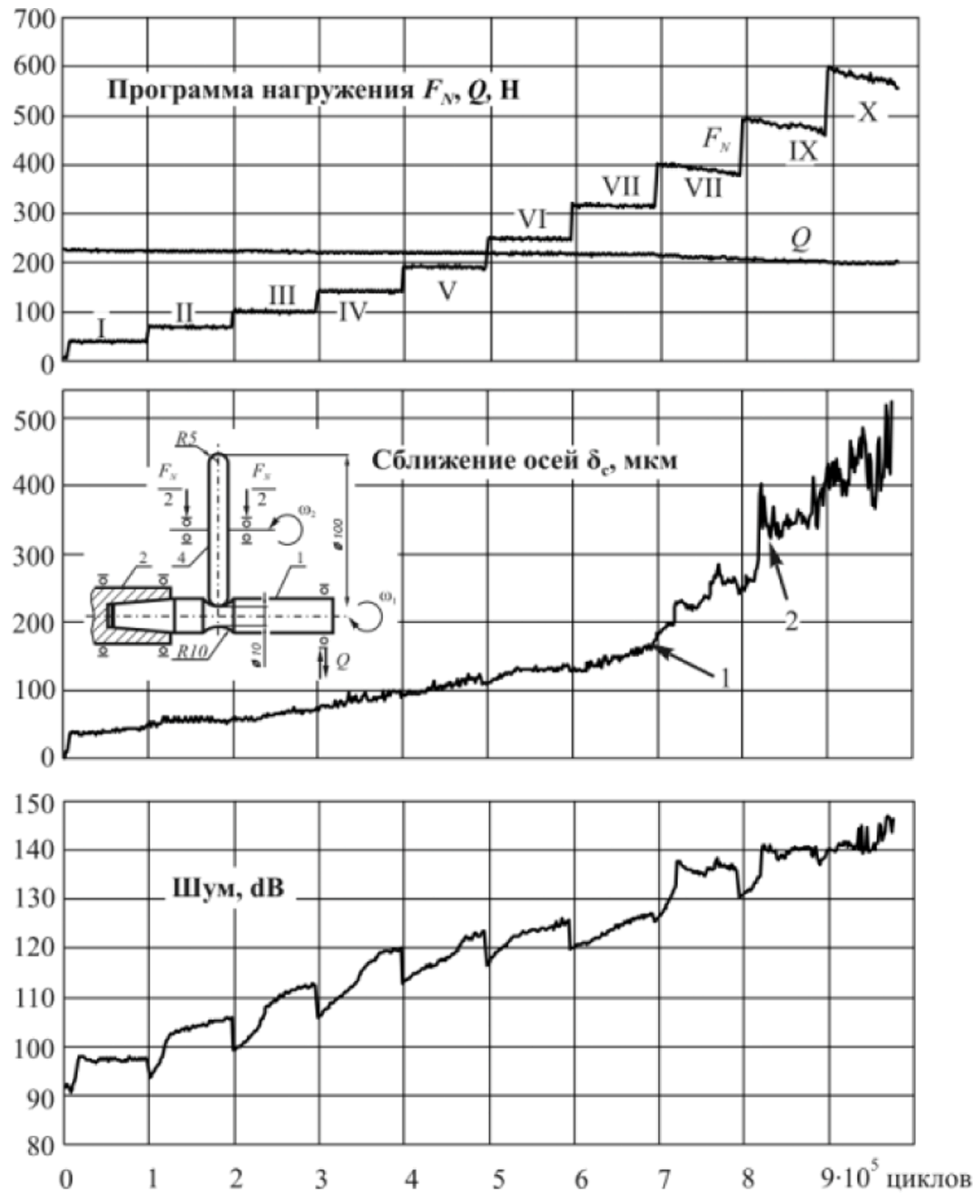


Fig. 12. Test protocol for contact-mechanical fatigue of the roller (25CrMnTi steel) - shaft (C45 steel) system [25].

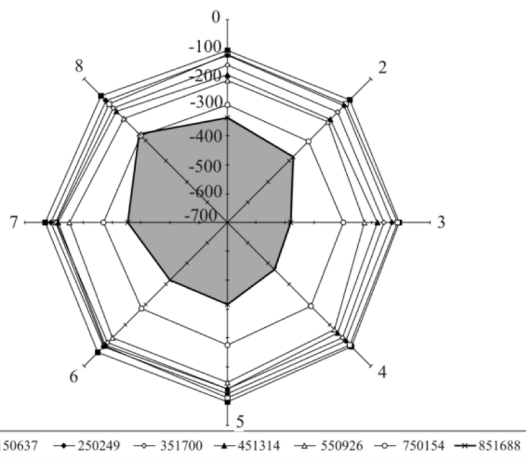


Fig. 13. Variation of radial residual deformation (μm) as a function of the number of loading cycles at 8 points along the shaft diameter [26].

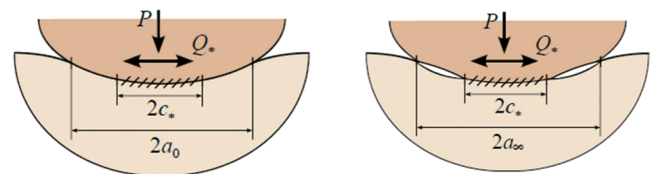


Fig. 14. Initial and final configurations of the considered contact pair contact area.

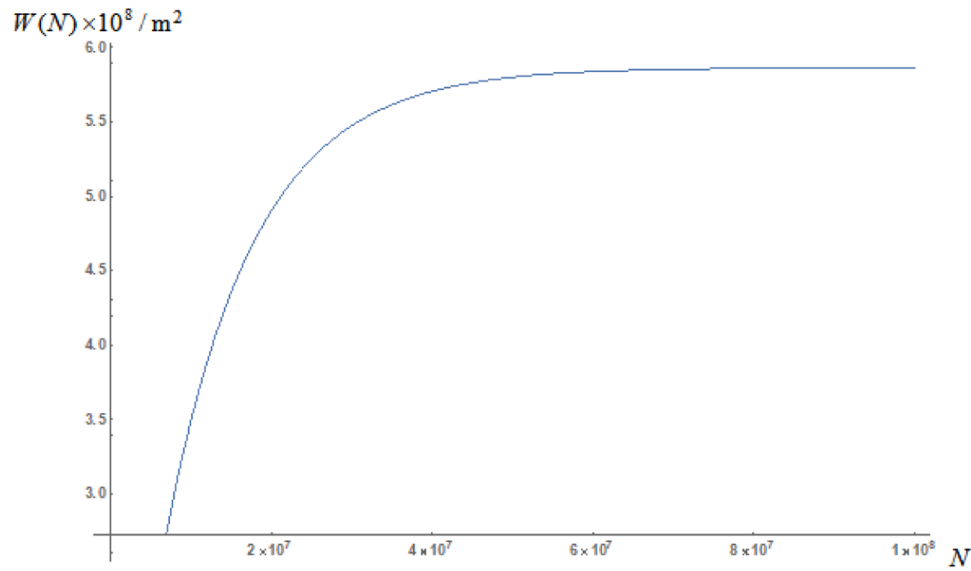
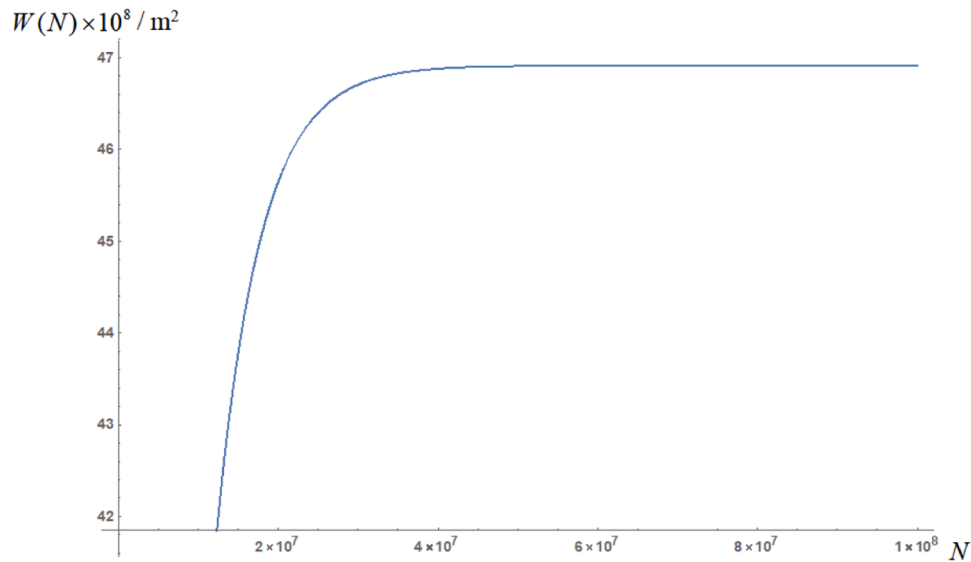
The a_0 is determined by the following formula:

$$a_0 = \frac{4RP}{\pi E^*} \quad (2)$$

where E^* is effective elastic modulus in the contact area:

$$E^{*-1} = (1 - \nu_1^2)E_1^{-1} + (1 - \nu_2^2)E_2^{-1} \quad (3)$$

Here E_i , ν_i are the Young's modulus and Poisson's ratio for the corresponding material of the two bodies in contact.

Fig. 15. Wear $W(N)$ under normal load $P = 50$ kN.Fig. 16. Wear $W(N)$ under normal load $P = 200$ kN.

The wear function as a number of cycles function is represented as follows:

$$W(N) = W_{\infty}(1 - \exp(-N/N_1)) \quad (4)$$

where N_1 is free parameter to be defined.

The final wear is determined by the formula:

$$W_{\infty} = 2 \int_{c^*}^{a_{\infty}} w_{\infty}(x) dx = \frac{c^* a_0^2}{R} \left(\frac{2}{3} \left(\frac{a_{\infty}}{c^*} \right)^2 \chi^2 + \frac{\chi^2}{3} - 1 \right) \sqrt{\left(\frac{a_{\infty}}{c^*} \right)^2 - 1} \quad (5)$$

The limit half-width of the contact zone a_{∞} is obtained from the equation $w_{\infty}(a_{\infty}) = 0$ and the dimensionless parameter χ is: [28]

$$\chi^2 = 1 - \frac{Q^*}{Pf} \quad (6)$$

Differentiating (4) by the variable “number of cycles”, we obtain::

$$\frac{dW}{dN} = \frac{W_{\infty}}{N_1} \exp\left(-\frac{N}{N_1}\right) \quad (7)$$

On the other hand: [27]

$$\frac{dW}{dN} = \frac{2K_w}{f} E_N(c^*) \quad (8)$$

$$\frac{dW}{dN} = \frac{2K_w}{f} E_N(c^*) \quad (9)$$

Omitting a number of transformations presented in [28], we obtain the expression for N_1 :

$$N_1 = fW_{\infty}/2K_w E_0(c^*) \quad (10)$$

Formula (10) allows us to calculate the amount of wear defined by the formula (4) as a function of the cycles number.

As an example Figs. 15, 16 show plots of the of the wear value $W(N)$ on the cycles number dependence for different values of the normal load under conditions of contact between the roller and the conductor.

Note that using the proposed approach requires modification of the algorithm to ensure that it can be applied to the experimental conditions described in this section. For this purpose, it is necessary to modify the

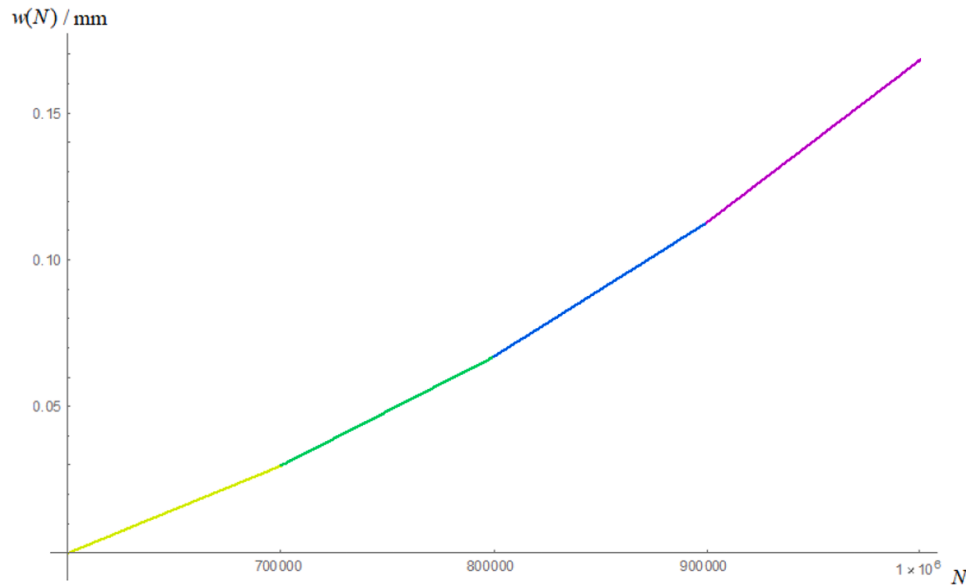


Fig. 17. Wear depth $w(N)$, mm.

model taking into account multi-cycle contact wear under the influence of a variable (instead of constant, as in the initial formulation) normal load specified in accordance with the scheme shown in Fig. 12.

In the practical implementation of the described algorithm for calculating the amount of wear depending on the number of cycles, the following value is used

$$\chi = \sqrt{1 - Q_*/fP} \quad (11)$$

where Q_* and P are the tangential and normal loads respectively, f is friction coefficient [28].

It is easy to notice that this value will have a complex value under the following condition $Q_*/fP > 1$. Until this value becomes real it is assumed that the roller-shaft system deforms in the elastic regime and the fatigue strain values are negligible. This fact is confirmed by analyzing the axis convergence diagram in Fig. 12. It can be noticed that the convergence of axes up to VII loading step is almost linear, and from the end of VII step there is a significant increase in the convergence of axes with the appearance of “beats” due to the significant accumulation of fatigue deformations and changes in the contact area geometry shape.

Thus, at each loading stage of the contact wear under partial fretting conditions problem is solved and the next values are defined:

$W(N) = W_\infty(1 - \exp(-N/N_1))$ is wear value depending on the number of cycles;

$a(N) = a_\infty - (a_\infty - a_0)\exp(-N/N_1)$ is contact zone half-width;

$w(N) = \frac{a^2(N)}{6R} - \frac{\chi^2}{2R} + \frac{K_w \Delta x}{a(N)} PN + \frac{2P}{\pi E^*} \left(\frac{3}{2} - \ln 2 - l\left(\frac{\chi}{a(N)}\right) \right)$ is wear distribution depth, $l(\xi) = 1 - \frac{1}{2} \ln \frac{1}{1-\xi^2} + \frac{\xi}{2} \ln \frac{1-\xi}{1+\xi}$.

For comparison with the experimental results, the value of the wear depth corresponding to the shaft radial residual deformation obtained at eight of its points is of interest (Fig. 13).

The results of concerned problem solution are shown in Fig. 17 for a given loading history (different colors indicate loading steps starting from VII):

As can be noticed from Figs. 13 and 17 that there is a certain correlation between the values of fatigue strains observed experimentally and obtained by model calculations. From a comparison of Figs. 13 and 17, it follows that the experiment radial residual strains of 0.3–0.4 mm, while the modelling studies give values for radial residual strains of approximately 0.17 mm. This fact can be explained by the assumption of fatigue deformations in the roller absence, which was adopted during the mechanical-mathematical model development. Also, it is worth

noting that the model proposed by Jäger [28], which is used in carrying out DT simulations, does not take into account the impact of temperature effects which have a significant influence on the stress-strain state of the system elements during contact interaction tests [25,26].

Thus, the general scheme of the developed mine hoisting complex elements digital twin work organization can be presented in Fig. 18.

When developing and setting up the DT, the SQL database (containing data coming from system for monitoring mine lifting vessel motion smoothness) and finite-element software complex Ansys Workbench (numerical modeling of the contact interaction of the roller with the conductor performance) were used. In addition, the computer algebra system Wolfram Mathematica was actively used to develop an algorithm for determining the force impact of the roller on the conductor using data from system for monitoring mine lifting vessel motion smoothness, as well as in the development of algorithms for calculating the fatigue wear of the conductor and their verification using data from field observations).

It is important to note, the input to the DT is dataset on the state of the mine lifting vessel, all other modules that make up the DT, make calculations in automatic mode.

5. Conclusions

The article presents a description of the mine lifting complex elements DT development process. In particular the geotechnical system “roller of the lifting vessel - mine conductor” DT is considered. The developed DT allows to determine the moving lifting vessel on mine conductors contact interaction forces in real time using data from the motion smoothness monitoring system. The obtained forces values allow us to calculate both the current conductors under the influence of the moving lifting vessel stress-strain state and the number of cycles “descent-lift” to conductors fatigue wear.

There are some conclusions observed from the results of system under consideration DT wear numerical simulations:

- (1) When a single roller interacts with the conductor, the following relationship is observed. When friction is taken into account, the number of cycles to fatigue failure of the conductor decreases significantly for any combination of mean stress and stress component correction methods;

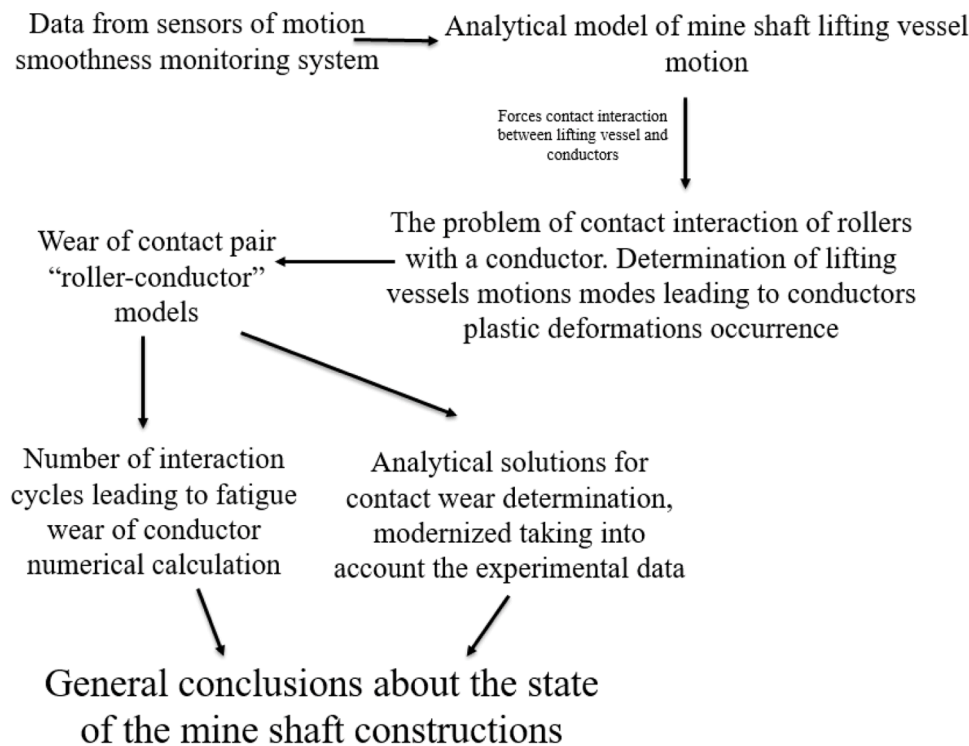


Fig. 18. General scheme of the digital twin.

- (2) When two rollers interact with the conductor, the number of cycles to fatigue failure decreases comparing to the number of cycles values when the conductor interacts with a single roller;
- (3) The number of cycles before fatigue cracks occur in the conductor for the case of contact with friction is greater than for contact without friction when two rollers impact the conductor. This is caused by the fact that the zone of stress concentration and, as a consequence, the area of fatigue crack initiation is the contact zone of the roller with the conductor in the case of interaction with a single roller. Therefore, the stress concentration in the contact zone increases as the friction coefficient increases. At the same time, the fatigue wear initiation region is outside the contact zone in the case of impact from two rollers. Thus, when the friction coefficient increases the values of deformations and, as a consequence, stresses in the zone of their maximum concentration decrease in the case of contact of a conductor with two rollers.

Modification of the mechanical-mathematical model of contact wear presented by Argatov is performed. The variation of the normal load as a function of the loading cycle is taken into account. The developed mechanical-mathematical model of multi-cycle DT wear is verified by the experimental investigations and can be refined with a set of statistics of the considered physical object observations. By comparing the fatigue strain values observed in experimental tests with those calculated from the model, a certain correlation and discrepancy between the two were identified. The discrepancy can be attributed to the assumption of neglecting fatigue deformation of the rollers when establishing the mechanical mathematical model.

The digital twin developed makes it possible to provide additional monitoring of the mine shaft steel structures under various operating conditions state, which makes it possible to rely not only on visual monitoring means. This fact not only minimizes costs, but also ensures safe operation of the geotechnical system under consideration. In addition, the DT of mine lifting complex elements allows performing computer modelling of lifting vessel motion various scenarios, which

makes it possible to determine the optimal motion modes with maximum speed.

The disadvantages of the developed DT include the complexity of its verification in real "roller of the lifting vessel - mine conductor" system operational conditions due to the complexity of conductor wear monitoring in the process of the mine lifting complex operation.

In the context of further research, it is planned to refine the models underlying the DT, taking into account different input data, considering the peculiarities of the mine hoisting complex state monitoring system. It is also planned to collect mine hoisting statistics and further verification of the mine hoisting systems developed DT operation using intelligent processing of hoisting data using machine learning techniques.

CRediT authorship contribution statement

Michael A Zhuravkov: Writing – review & editing, Supervision. **Mikhail A Nikolaichik:** Writing – original draft, Methodology. **Zengcheng Wang:** Software. **Guangbin Yu:** Project administration.

Declaration of competing interest

The authors declare that they have no known competing financial interests or personal relationships that could have appeared to influence the work reported in this paper.

Funding

This work was supported by Major Science and Technology Projects of Heilongjiang Province Unveils Project (2022ZXJ01A02, 2022ZXJ01A01) and Projects of the Spring Goose Support Program of Heilongjiang Province (CYCX24011).

Data availability

No data was used for the research described in the article.

References

- [1] X. Liu, D. Jiang, B. Tao, F. Xiang, G. Jiang, Y. Sun, J. Kong, G. Li, A systematic review of digital twin about physical entities, virtual models, twin data, and applications, *Adv. Eng. Inform.* 55 (2023) 101876, <https://doi.org/10.1016/j.aei.2023.101876>.
- [2] B. Hickey, D.C. Gachon, D.J. Cosgrove, Digital Twin – A tool for project management in manufacturing, *Procedia Comput. Sci.* 217 (2023) 720–727, <https://doi.org/10.1016/j.procs.2022.12.268>.
- [3] M. Attaran, B.G. Celik, Digital Twin: benefits, use cases, challenges, and opportunities, *Decis. Anal. J.* 6 (2023) 100165, <https://doi.org/10.1016/j.dajour.2023.100165>.
- [4] C. Cimino, E. Negri, L. Fumagalli, Review of digital twin applications in manufacturing, *Comput. Ind.* 113 (2019) 103130, <https://doi.org/10.1016/j.compind.2019.103130>.
- [5] S. Torregrosa, V. Champaney, A. Ammar, V. Herbert, F. Chinesta, Predicting high-fidelity data from coarse-mesh computational fluid dynamics corrected using hybrid twins based on optimal transport, *Mech. Ind.* 25 (2024), <https://doi.org/10.1051/meca/2024023>.
- [6] X. Hu, X. Liu, Y. Luo, Analytical design of optimal fractional order PID control for industrial robot based on digital twin, in: *2022 IEEE 2nd International Conference on Digital Twins and Parallel Intelligence (DTPi)*, 2022, pp. 1–6.
- [7] H. Gui, Z. Zhao, Research on obstacle climbing gait structure design and gait control of hexapod wall climbing robot based on STM32F103 core controller, *Mech. Ind.* 24 (2023), <https://doi.org/10.1016/j.compind.2019.103130>.
- [8] S.O. Farah, M. Guessasma, E. Bellenger, Digital twin by DEM for ball bearing operating under EHD conditions, *Mech. Ind.* 21 (2020), <https://doi.org/10.1051/meca/2020022>.
- [9] S. Patalano, F. Vitolo, A. Lanzotti, Automotive power window system design: object-oriented modelling and design of experiments integration within a digital pattern approach, *Mech. Ind.* 6 (2016), <https://doi.org/10.1051/meca/2015104>.
- [10] S. Schmid, D. Kaufmann, U. Dahmen, F. Eggers, I. Valais, K.-U. Schröder, J. Roßmann, Force and stress simulation in experimentable digital twins using the transfer matrix method, *Appl. Mech.* 6 (2025), <https://doi.org/10.3390/applmech6010008>.
- [11] U. Dahmen, J. Rossmann, Experimentable digital twins for a modeling and simulation-based engineering approach, <https://doi.org/10.1109/syseng.2018.8544383>.
- [12] N.K. Kuznetsov, S.V. Eliseev, A. Yu Perelygina, Reduction of dynamic loads in mine lifting installations, *J. Phys. Conf. Ser.* 944 (2018) 012070, <https://doi.org/10.1088/1742-6596/944/1/012070>. –012070.
- [13] Vladimir Samusia, Inna Iliina, S. Iliina, Computer modeling and investigation of dynamics of system “vessel–reinforcement” in shafts with broken geometry, *Bull. PNRPU. Geol. Oil Gas Eng. Min.* 20 (2016) 277–285, <https://doi.org/10.15593/2224-9923/2016.20.8>.
- [14] R. Wu, Z. Zhu, G. Cao, Computational fluid dynamics modeling of rope-guided conveyances in two typical kinds of shaft layouts, *PLOS ONE* 10 (2015) e0118268, <https://doi.org/10.1371/journal.pone.0118268>.
- [15] Y. Guo, D. Zhang, X. Zhang, S. Wang, W. Ma, Experimental study on the nonlinear dynamic characteristics of wire rope under periodic excitation in a friction hoist, *Shock Vib.* 2020 (2020) 1–14, <https://doi.org/10.1155/2020/8506016>.
- [16] V. Pershin, Aleksandr Kopytov, A. Wetti, Research in the impact of dynamic loads for the development of Pentice designs when sinking skip shafts, *E3S Web Conf.* 105 (2019) 01056, <https://doi.org/10.1051/e3sconf/201910501056>. –01056.
- [17] S. Wolny, F. Matachowski, Analysis of loads and stresses in structural elements of hoisting installations in mines, *Eng. Trans.* 58 (2010) 153–174.
- [18] M. Zhuravkov, Y. Lyu, Eduard Starovoitov, *Mechanics of Solid Deformable Body*, Springer Nature, 2023.
- [19] M. Nikolaitchik, Determination of the skip force effect on guides in mine shaft, *E3S Web Conf.* 201 (2020) 01017, <https://doi.org/10.1051/e3sconf/202020101017>. –01017.
- [20] M.A. Zhuravkov, V. Savchuk, M.A. Nikolaitchik, Analytical model of skip motion taking into account influence of head and balancing ropes, *J. Belarusian State Univ. Math. Inform.* (2021) 105–113, <https://doi.org/10.33581/2520-6508-2021-2-105-113>.
- [21] S. Timoshenko, *Theory of elasticity*, McGraw-Hill, Auckland, London, 1970.
- [22] V.L. Popov, *Contact Mechanics and Friction*, Springer Berlin Heidelberg, Berlin, Heidelberg, 2017, <https://doi.org/10.1007/978-3-662-53081-8>.
- [23] S.-P. Zhu, Q. Lei, H.-Z. Huang, Y.-J. Yang, W. Peng, Mean stress effect correction in strain energy-based fatigue life prediction of metals, *Int. J. Damage Mech.* 26 (2016) 1219–1241, <https://doi.org/10.1177/1056789516651920>.
- [24] A. Nadai, P.G. Hodge, *Theory of Flow and Fracture of Solids*, vol. II, J. Appl. Mech. 30 (1963) 640, <https://doi.org/10.1115/1.3636654>. –640.
- [25] L.A. Sosnovslii, S.S. Shcherbakov, Formation of residual wavefor surface damages at mechanorolling fatigue, *Bull. BSUT: Sci. Transp.* 2 (2005) 71–87.
- [26] O.M. Elovoy, *Mechanical Engineering: Interdisciplinary Collection of Scientific Works*, 23, BNTU, Minsk, 2007, pp. 270–275.
- [27] I.I. Argatov, JoonWoo Bae, YoungSuck Chai, A simple model for the wear accumulation in partial slip hertzian contact, *Int J. Appl. Mech.* 12 (2020) 2050074, <https://doi.org/10.1142/s175882512050074x>. –2050074.
- [28] J. Jäger, Half-planes without coupling under contact loading, *Arch. Appl. Mech.* 67 (1997) 247–259, <https://doi.org/10.1007/s004190050115>.